What's the Magic Word? A Control Theory of LLM Prompting

Anonymous Authors[1]

Abstract

Prompt engineering is crucial for deploying LLMs but is poorly understood mathematically. We formalize LLM systems as a class of discrete stochastic dynamical systems to explore prompt engineering through the lens of control theory. We offer a mathematical analysis of the limitations on the controllability of self-attention as a function of the singular values of the parameter matrices. We present complementary empirical results on the controllability of a panel of LLMs, including Falcon-7b, Llama-7b, and Falcon-40b. Given initial state $\mathbf{x}_0$ from Wikitext and prompts of length $k \leq 10$ tokens, we find that the "correct" next token is reachable at least 97% of the time, and that the top 75 most likely next tokens are reachable at least 85% of the time. Intriguingly, short prompt sequences can dramatically alter the likelihood of specific outputs, even making the least likely tokens become the most likely ones. This control-theoretic analysis of LLMs demonstrates the significant and poorly understood role of input sequences in steering output probabilities, offering a foundational perspective for enhancing language model system capabilities.

1. Introduction

LLMs pre-trained on unsupervised next token prediction objectives exhibit unprecedented dynamic reprogrammability achieved through "prompting", often referred to as zero-shot learning (Brown et al., 2020; Wei et al., 2022; Hagendorff, 2023; Noever & McKee, 2023; OpenAI, 2023; 2022). These capabilities appear to emerge as the model's size, training data, and training time are scaled. The dynamic reprogrammability of LLMs is akin to the adaptable computational capacities observed in biological systems. This feature finds applications across domains such as machine translation (Wang et al., 2023a), code generation (Rozière et al., 2023), and chatbots (Bai et al., 2022). A rigorous understanding of the prompt's influence over LLM generation would be of great utility for understanding LLMs and building more robust and capable systems leveraging LLMs.

Strategies for controlling pre-trained LLM generation today fall into three broad categories (Zhang et al., 2022):

1. **Input Optimization (Prompting):** Adjusting the input tokens (e.g., rewording the prompt) to improve subsequent text generation.
2. **Model Optimization:** Adjusting the weights of the network (e.g., fine-tuning, RLHF) to improve model behavior during inference.
3. **Post-processing:** Adjusting or re-ranking generated text (e.g., surrogate ranking algorithm).

Of all these approaches, input optimization (i.e., prompting) is the least invasive and lowest-cost method – and the least understood. Prompt optimization is also deeply connected to the zero-shot capabilities of LLMs – the mysterious emergent capabilities of LLMs such as problem-solving, knowledge retrieval, reasoning, and apparent general intelligence (Bubeck et al., 2023). With such a view, we seek to characterize the controllability of LLMs via prompting (Figure 1).

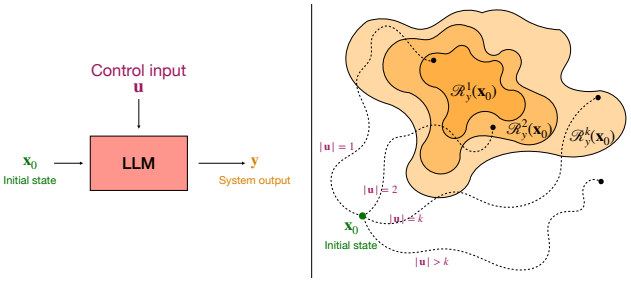

Figure 1. Illustration of the control-theoretic approach to LLM prompt engineering. **Left:** the LLM system's flow from an initial state $\mathbf{x}_0$ to a system output $\mathbf{y}$ under the influence of a control input $\mathbf{u}$ (all token sequences). **Right**: the reachable output sets $R_y^k(\mathbf{x}_0)$ for varying control input lengths k.

[1]Anonymous Institution, Anonymous City, Anonymous Region, Anonymous Country. Correspondence to: Anonymous Author <anon.email@domain.com>.

Preliminary work. Under review by the International Conference on Machine Learning (ICML). Do not distribute.

1.1. Contribution

We formalize LLM systems in the mathematical framework of control theory in Section 3. Our analysis focuses on the reachable set of outputs $\mathcal{R}_y(\mathbf{x}_0)$ for an LLM system. The reachable set is a fundamental concept in control theory that underlies notions of controllability, stability, and observability (cf. Appendix A). The reachable output set $R_y(\mathbf{x}_0)$ is the set of output sequences $\mathbf{y}$ for which there exists a control input sequence $\mathbf{u}^*$ that steers the LLM from initial state $\mathbf{x}_0$ to output $\mathbf{y}$ (cf. Definitions 3.3, A.5).

Our mathematical results in Section 4 prove an upper bound on the contents of the reachable output set for a self-attention head as a function of the singular values of its parameter matrices. Since self-attention is the only component in a transformer block where significant information is exchanged between token representations, this bound provides a foothold for analysis of LLM controllability from the perspective of mechanistic interpretability (e.g., (Bricken et al., 2023; Chefer et al., 2021; Conmy et al., 2023)). Moreover, this bound represents a necessary condition for an output to be in the reachable set.

Our empirical results apply state-of-the-art prompt optimization techniques (Section 5.1) to demonstrate a lower bound on the contents of the reachable output set for a panel of LLMs, including Llama-7b (Touvron et al., 2023), Falcon-7b, and Falcon-40b (Almazrouei et al., 2023). Specifically, we sample initial states $\mathbf{x}_0$ from the Wikitext dataset (Merity et al., 2016) and probe the reachable output tokens y under length-constrained control input sequences $\mathbf{u} : |\mathbf{u}| \leq k$. The length constraint k is highly relevant for *optimal control* of LLMs, as prompts with fewer tokens require fewer computation and memory resources. We find that the reachable output set contains the "correct" next Wikitext token following $\mathbf{x}_0$ over 97% of the time with prompts of $k \leq 10$ tokens. We expand our analysis of the contents of $R_y(\mathbf{x}_0)$ by sampling target output tokens y based on the LLMs initial estimate of output likelihood $P_{LM}(y|\mathbf{x}_0)$. We find that the top 75 most likely output tokens y are reachable at least 85% of the time with prompts of $k \leq 10$ tokens. Intriguingly, some tokens drawn from the set of *least* likely outputs are controllable to the most likely output with $k \leq 4$ control input tokens. Our results suggest that prior likelihood-based metrics, such as cross-entropy loss, cannot guarantee exclusion from the reachable set, emphasizing the gap in our current understanding of LLM systems and control. Implications of our results and open questions in LLM control theory are further discussed in Section 6.

2. Related Work

Much of the work on prompt optimization is concerned with finding prompts that induce higher LLM performance on "fill-in-the-blank" or "cloze" tasks (Taylor, 1953). One can frame a range of tasks including knowledge retrieval (Petroni et al., 2019), reasoning (Weston et al., 2016), and sentiment analysis (Wang et al., 2023b) as fill-in-the-blank tasks:

- **Knowledge Retrieval:** *"The Titanic sank in the year **[MASK]**."* (Answer: "1912")
- **Reasoning:** *"A is taller than B. B is taller than C. Is A taller than C? **Answer: [MASK]**"* (Answer: "Yes")
- **Sentiment Analysis:** *"I am sad today. **The sentiment of the previous sentence was [MASK]**"* (Answer: "Negative")

Notably, there is some freedom in the bolded "prompt text" that surrounds the question to convert it into a "fill-in-the-blank" task. As it turns out, the prompt tokens have a large effect on LLM performance (Brown et al., 2020; Zhang et al., 2022; Jiang et al., 2020).

Modern prompt optimization algorithms generally consist of two iterated steps: a sampling step where new prompts are generated and a testing step where the utility of the new prompts is evaluated, and the best are selected for the next iteration. Algorithms primarily differ in the sampling procedure, where various heuristics may be used to pick high-value swaps (Wen et al., 2023; Zhou et al., 2023; Reynolds & McDonell, 2021). Overall, AutoPrompt and its derivative algorithms have been the most numerically successful prompt optimization methods, with the greedy coordinate gradient (GCG) algorithm having state-of-the-art performance (Zou et al., 2023).

The AutoPrompt Family: AutoPrompt (Shin et al., 2020) pioneered the current wave of prompt optimization. Shin *et al* propose a prompt optimization technique and demonstrate its effectiveness for engineering prompts to improve LLM performance on knowledge and sentiment analysis tasks. At its core, the AutoPrompt algorithm leverages gradient information at the token embedding layer to inform iterative token exchanges within the prompt. This method was extended in (Zou et al., 2023) as the greedy coordinate gradient (GCG) algorithm. Taking inspiration from adversarial examples (Goodfellow et al., 2015), Zou *et al* applied this AutoPrompt variant to generate "jailbreak" prompts that cause aligned LLMs to generate objectionable content.

Other Prompt Optimization Methods: Other investigations on LLMs as prompt optimizers (Zhou et al., 2023) and further analysis of manual prompt optimization (Reynolds & McDonell, 2021) are informative but do not exceed the AutoPrompt family's performance. Some other methods include GBDA (Guo et al., 2021), an approach based on

the Gumbel-Softmax reparametrization, the PEZ algorithm (Wen et al., 2023), which directly optimizes embeddings via gradient information, and FluentPrompt (Shi et al., 2022), which differs from AutoPrompt by incorporating Langevin dynamics. Despite the variety of alternatives, GCG retains state-of-the-art performance.

Control Theory for LLMs: To our knowledge, the only other work to date on the controllability of LLMs is (Soatto et al., 2023). Soatto et al analyze the controllability of LLMs in terms of "meaningful sentences", defined as the sigma-algebra generated by snippets of text written on the Internet. Their empirical analysis revolves around demonstrating that LLMs are capable of attributing meaning. The theoretical analysis of LLM controllability is limited to "meaningful sentences", eliminating the possibility of out-of-distribution inputs and outputs. These restrictions render their results challenging to leverage toward a practical understanding of LLM controllability. As stated in Section 5.5 of (Soatto et al., 2023), "If fed gibberish, the well-trained bot operates out of distribution, which does not allow predicting the reachable set". We situate our work as a practically oriented exploration of LLM controllability. Motivated by challenges in developing LLM systems, we do not eliminate "meaningless sentences" from the state space or input space. We aim to establish a rigorous, general framework for understanding LLM systems and controllability that is amenable to the development of theory and practical engineering insights on systems design.

3. Control Theory for LLMs

Control theory originates from the study of automatic control systems in engineering. It seeks to understand how a "plant" system can be influenced toward a desired state using a "control signal" – often in the presence of disturbances and uncertainty.

Control theory is central to a variety of engineering problems, from electrical engineering to autopilot to telecommunications to manufacturing. Surprisingly, control theory has also been highly applicable to a diverse range of scientific disciplines. Analyzing systems through the lens of controllability has proven fruitful for generating insight into biological systems such as cell signaling pathways and neural networks (Yi et al., 2000), the economics of central banking (Aniţa et al., 2011), and controlling the spread of infectious diseases (Roy et al., 2009). One of the central benefits of studying systems via controllability is that a range of questions and problems naturally emerge from the framing: *when is control possible? What is the cost of control? How computationally intensive is control?* These questions are both practically useful and often lead to fundamental insights about the nature of the system in question.

To develop a control theory of LLMs, we provide fundamental abstract definitions of systems and control (Appendix A). We apply them to define LLM systems and outline specific canonical control concepts and problems such as controllability and reachability that arise naturally for LLM systems.

Language Model Notation: We denote a causal language model using P_{LM}. P_{LM} maps from an ordered list of tokens from a vocabulary set $\mathcal{V}$ (e.g., $\mathbf{x} \in \mathcal{V}^n$) to the probability distribution over the next token $P_{LM}(x_{n+1}|\mathbf{x}) \in [0,1]^{|\mathcal{V}|}$. We use $\mathcal{V}^*$ to denote the set of all possible sequences of any length composed of tokens from $\mathcal{V}$. The addition operator indicates the concatenation of token sequences. Bolded lowercase variables (e.g., $\mathbf{x} = [x^1, \ldots, x^n]$) denote token sequences while unbolded lowercase variables refer to individual tokens (e.g., $x \in \mathcal{V}$). The length of a token sequence is denoted $|\mathbf{x}|$.

While LLMs are at times leveraged in a manner that masks the iterative aspects of generation, the reality is that token generation and externally imposed "control input" sequences are generated and processed sequentially, leading to non-trivial system dynamics. Several key differences remain between LLM-based systems and systems typically modeled through ordinary differential equations (ODEs), which have long been a cornerstone in the study of continuous-time dynamical systems:

1. **Discrete state and time:** LLM systems operate on sequences of discrete tokens over a discrete time set, in contrast to the continuous state spaces and time sets studied in classical control theory.
2. **Shift-and-Grow State Dynamics:** Whereas the system state in an ODE-based system has a fixed size over time, the system state $\mathbf{x}(t)$ for LLM systems grows as tokens are added to the state sequence.
3. **Mutual exclusion on control input token vs. generated token:** The LLM system state $\mathbf{x}(t)$ is written to one token at a time. The newest token is either drawn from the control input $u(t)$ or is generated by the LLM by sampling $x' \sim P_{LM}(x'|\mathbf{x}(t))$. This differs from traditional discrete stochastic systems, where the control sequence and internal dynamics generally affect the state synchronously.

We begin by rigorously defining LLM systems with user input, drawing from the abstract mathematical definition of a system (Definition A.1).

Definition 3.1 (LLM System with Control Input)**.** An autoregressive LLM system with control input $\Sigma = (\mathcal{V}, P_{LM})$ consists of:

- $\mathcal{T} = \mathbb{N}$ – The **time set** is the natural numbers.

- $\mathcal{X} = \mathcal{V}^*$ – The **state space** consists of all possible token sequences of any length drawn from $\mathcal{V}$. We denote the state at time t as $\mathbf{x}(t) = [x^0(t), \ldots, x^t(t)]$.
- $\mathcal{U} = \mathcal{V} \cup \varnothing$ – The **input** takes values from the vocabulary set $\mathcal{V}$ or null.
- $\phi : \mathcal{X} \times \mathcal{U} \times \mathcal{T}^2 \to \mathcal{X}$ – The **transition map** is

$$\phi(\mathbf{x}(t), u(t), t, t+1) = \begin{cases} \mathbf{x}(t) + u(t) & \text{if } u(t) \neq \varnothing \\ \mathbf{x}(t) + x' & \text{else} \end{cases} \tag{1}$$

  where $x' \sim P_{LM}(x'|\mathbf{x}(t))$. Note that the general multi-step transition map $\phi(\mathbf{x}(t), u, t, t+N)$ can be achieved by iterating equation 1 for control sequences $\mathbf{u}$ defined over the interval $[t, t+N]$.
- $h(\mathbf{x}(t); r) = [x^{t-r}(t), \ldots, x^t(t)]$ – The **readout map** returns the most recent r tokens from state $\mathbf{x}(t)$.

We note that this LLM system definition is generalizable to a variety of LLM augmentation, including chain-of-thought (Wei et al., 2023), retrieval-augmented generation (Lewis et al., 2020), and chatbot interaction. For example, chain-of-thought is equivalent to sampling the readout map $h(x(t), r)$ at time $T > |\mathbf{u}| + |\mathbf{x}_0| + r$ for prompt $\mathbf{u}$ and initial state $\mathbf{x}_0$. A similar formulation may be applied to LLM systems endowed with programmatic tools (e.g., (Patil et al., 2023)).

In Definition 3.1, we assume that the control input gets to "decide" whether to yield token generation to the LLM ($u(t) = \varnothing$) or override the LLM and add some token $u(t) \neq \varnothing$ to the state $\mathbf{x}(t)$. This assumption generally holds when building LLM systems, though it may not hold when using existing systems (e.g., via non-streaming API). When discussing finite-length control inputs – e.g., the family of k-long input sequences $\mathbf{u} \in \mathcal{V}^k$ – the value of $u(\ell) : \ell > k$ is implicitly $\varnothing$ unless otherwise stated.

While next token generation $x' \sim P_{LM}(x'|\mathbf{x}(t))$ in equation 1 is probabilistic, we may render the system deterministic by sampling with zero temperature (i.e., greedy decoding). The greedy decoding assumption provides a foothold to analyze the reachable sets and controllability of LLM systems without invoking notions of stochastic control as in (Sivaramakrishnan et al., 2023; Soatto et al., 2023). Moreover, it remains connected to temperature-based stochastic decoding strategies as a limiting case of temperature-based sampling as zero-temperature sampling.

We now extend Definition A.4 to define output controllability for LLM systems:

Definition 3.2 (LLM Output Reachability)**.** Output token sequence $\mathbf{y} \in \mathcal{V}^r$ is reachable from initial state $\mathbf{x}_0 \in \mathcal{V}^*$ for LLM system $\Sigma(\mathcal{V}, P_{LM})$ iff there exists some time T and input $\mathbf{u}^* \in \mathcal{U}^T$ that steers the LLM from initial state $\mathbf{x}_0$ to output $\mathbf{y} = h(\mathbf{x}(T), r)$ at time T.

We disregard the trivial solution wherein the control input $\mathbf{u}^*(t)$ overrides the LLM to force the state sequence to take on the desired output value $\mathbf{y}$.

The reachable output set definition for LLM systems follows from Definition A.5:

Definition 3.3 (LLM Reachable Output Set)**.** The reachable output set from initial state $\mathbf{x}_0 \in \mathcal{V}^*$ for LLM system $\Sigma = (\mathcal{V}, P_{LM})$ is denoted $R_y(\mathbf{x}_0)$ and consists of all reachable outputs $\mathbf{y} \in \mathcal{V}^*$ from initial state $\mathbf{x}_0$.

Output controllability for LLMs follows from Definition A.7.

Definition 3.4 (LLM Output Controllability)**.** An LLM system $\Sigma = (\mathcal{V}, P_{LM})$ is output controllable iff, for every initial state $\mathbf{x}_0 \in \mathcal{V}^*$, the reachable output set $\mathcal{R}_y(\mathbf{x}_0) = \mathcal{V}^*$.

The turn-based nature of writing to the LLM state sequence $\mathbf{x}(t)$ invites the question of whether the prompt $\mathbf{u}$ should preempt the imposed state $\mathbf{x}_0$ or come after the state [1]. We focus our efforts on cases where $\mathbf{u}$ comes before imposed state sequence $\mathbf{x}_0$ due to its importance for developing system prompts and controlling text completion-based generation where the desired output is $\mathbf{x}_0 + \mathbf{y}^*$ for some desired continuation $\mathbf{y}^*$ of partial string $\mathbf{x}_0$. Due to the costly nature of long prompts, we are especially interested in the existence of prompts $\mathbf{u}^*$ with minimal length $|\mathbf{u}^*|$.

Definitions 3.3 and 3.4 form the basis for our control theory of LLMs. While amenable to theoretical analysis as in Section 4 and (Soatto et al., 2023), empirical analysis of the reachable set and controllability is challenging due to the intractable size of $\mathcal{V}^*$. We propose the following statistical measure of controllability for practically assessing the controllability of an LLM system w.r.t. a dataset $\mathcal{D}$ under prompt length constraint $|\mathbf{u}| \leq k$:

Definition 3.5 ($k - \epsilon$ Controllability)**.** Consider a dataset of state-output pairs $\mathcal{D} = \{(\mathbf{x}_0^i, \mathbf{y}^i)\}_{i \in [N]}$. An LLM $\Sigma = (\mathcal{V}, P_{LM})$ is $k - \epsilon$ controllable w.r.t. $\mathcal{D}$ if

$$\Pr\{\mathbf{y} \notin \mathcal{R}_y^k(\mathbf{x}_0)\} \leq \epsilon \tag{2}$$

For $(\mathbf{x}_0, \mathbf{y}) \sim \mathcal{D}$, where $\mathcal{R}_y^k(\mathbf{x}_0^i)$ is the reachable set of outputs as in Definition 3.3 under the constraint that prompts $\mathbf{u}$ must have length $|\mathbf{u}| \leq k$.

[1] Both situations are reasonable in developing LLM systems: $\mathbf{u}$ preceding $\mathbf{x}_0$ may arise when prompting an LLM to complete a partial string $\mathbf{x}_0$. $\mathbf{u}$ proceeding $\mathbf{x}_0$ may arise when prompting an LLM in the presence of an imposed system prompt $\mathbf{x}_0$. Therefore, how an initial state $\mathbf{x}_0$ is interleaved with control input $\mathbf{u}$ is largely a design decision.

Our empirical work in Section 5.2 explores $k-\epsilon$ controllability w.r.t. initial states $\mathbf{x}_0$ sampled from the Wikitext dataset. While empirical analysis of LLM controllability is challenging due to the lack of apparent structure in LLM dynamics and the combinatorially large state space, we may still experimentally establish the *existence* of optimal prompts $\mathbf{u}^*$ that elicit a given output, and thus establish a lower bound on the content of the reachable set. Meanwhile, our theoretical work in Section 4 establishes upper bounds on the content of the reachable set for self-attention. We hope these complementary approaches aid in unifying our understanding of LLM systems.

4. Mathematical Analysis on the Controllability of Self-Attention

Self-attention is a central component in modern transformer-based language models (Brown et al., 2020; Touvron et al., 2023; Radford et al., 2019; Min et al., 2023). Introduced in (Bahdanau et al., 2016) and popularized by (Vaswani et al., 2017), self-attention is the primary component in transformers where token representations exchange information.

Definition 4.1 (Self-Attention)**.** Self-attention $\Xi = (\mathbf{W_q}, \mathbf{W_k}, \mathbf{W_v})$ is a map from $\mathbb{R}^{N\times d_{in}} \to \mathbb{R}^{N\times d_{out}}$ where N is an arbitrary number of input token representations each of dimensionality d_{in}, and d_{out} is the dimensionality of the output token representations.

$$\Xi(\mathbf{X}) = \mathbb{D}^{-1}\exp\left(\frac{\mathbf{Q}\mathbf{K}^\top}{\sqrt{d_k}}\right)\mathbf{V} \tag{3}$$

where $\exp()$ denotes element-wise exponentiation of the matrix entries, $\mathbf{W_q}, \mathbf{W_k} \in \mathbb{R}^{d_{in}\times d_k}$, $\mathbf{W_v} \in \mathbb{R}^{d_{in}\times d_{out}}$, $\mathbf{Q} = \mathbf{X}\mathbf{W_q}$, $\mathbf{K} = \mathbf{X}\mathbf{W_k}$, $\mathbf{V} = \mathbf{X}\mathbf{W_v}$, and $\mathbb{D}$ is a diagonal positive definite matrix defined as

$$\mathbb{D} = \text{diag}\left(\exp\left(\frac{\mathbf{Q}\mathbf{K}^\top}{\sqrt{d_k}}\right)\mathbf{1}_{N\times 1}\right) \tag{4}$$

where $\mathbf{1}_{N\times 1}$ is an $N\times 1$ matrix of ones.

Note that the parameters and operation of Ξ are independent of the number of token representations N. Self-attention is generally applied to discrete token sequences by embedding each token in the sequence as a vector in $\mathbb{R}^{d_{in}}$ to construct the matrix of N token representations $\mathbf{X} \in \mathbb{R}^{N\times d_{in}}$.

We are interested in the reachability of output token representations $\Xi(\mathbf{X}) \in \mathbb{R}^{N\times d_{out}}$, where we partition the input $\mathbf{X} \in \mathbb{R}^{(k+M)\times d_{in}}$ into an $k\times d_{in}$ block of control input representations $\mathbf{U}$ and an $M\times d_{in}$ block of imposed state representations $\mathbf{X}_0$ (cf. Definition 3.1). We also partition the output $\mathbf{X}' = \Xi(\mathbf{X}) \in \mathbb{R}^{(k+M)\times d_{in}}$ into a corresponding $k\times d_{out}$ matrix $\mathbf{U}'$ and an $M\times d_{out}$ matrix $\mathbf{Y}$. Motivated by the architecture of transformer-based language models, we seek to characterize the reachable set of output representations $\mathbf{Y} \in \mathcal{R}_y^k(\mathbf{X}_0)$ under imposed input representations $\mathbf{X}_0$ and controllable input representations $\mathbf{U}$, where $\mathbf{U}$ consists of k token representations. While the reachable set is now a set of continuous-valued output representation matrices in $\mathbb{R}^{M\times d_{in}}$, we may readily adapt Definition 3.3 to define the reachable set for these conditions.

Theorem 4.2 (Condition for Exclusion from the Reachable Set)**.** *A desired output representation $\mathbf{Y}^* \in \mathbb{R}^{M\times d_{out}}$ must be excluded from the reachable set $\mathcal{R}_y^k(\mathbf{X}_0)$ if the following condition holds for any row i:*

$$\|\mathbf{y}^{*i} - \frac{\hat{D}^i_{xx}}{\hat{D}^i_{xx} + k\exp\left(\frac{\Omega_x\sigma_q\sigma_k\Omega_u}{\sqrt{d_k}}\right)}\hat{\mathbf{y}}^i_x\| \le \sigma_q\Omega_u \tag{5}$$

and $\langle \mathbf{y}^{*i}, \hat{\mathbf{y}}^i_x\rangle \le 0$, where $\Omega_u = \max_j \|\mathbf{u}^j\|$ for rows $\mathbf{u}^j$ of $\mathbf{U}$, $\Omega_x = \max_j \|\mathbf{x}_0^j\|$ for rows $\mathbf{x}_0^i$ of $\mathbf{X}_0$, σ_q and σ_k are the maximum singular values of $\mathbf{W_q}, \mathbf{W_k}$ respectively, $\hat{D}^i_{xx}$ is the ith element on the diagonal of $\hat{\mathbf{D}}_{xx}$, which is given by

$$\hat{\mathbf{D}}_{xx} = \textit{diag}\left(\exp\left(\frac{\mathbf{Q_x}\mathbf{K_x}^\top}{\sqrt{d_k}}\right)\mathbf{1}_{M\times 1}\right), \tag{6}$$

$\mathbf{y}^{*i}$ is the ith row of $\mathbf{Y}^*$, and y^i_x is the ith row of $\hat{\mathbf{Y}}_x$, which is given by

$$\hat{\mathbf{Y}}_x = \hat{\mathbf{D}}^{-1}_{xx}\exp\left(\frac{\mathbf{Q_x}\mathbf{K_x}^\top}{\sqrt{d_k}}\right)\mathbf{V}_x \tag{7}$$

where $\mathbf{Q_x} = \mathbf{X_0}\mathbf{W_q}$, $\mathbf{K_x} = \mathbf{X_0}\mathbf{W_k}$, and $\mathbf{V_x} = \mathbf{X_0}\mathbf{W_v}$

The proof of Equation 5 is provided in Appendix B.

The proof revolves around decomposing the output representations $\mathbf{Y}$ into two components $\mathbf{Y}_x$ and $\mathbf{Y}_u$ composed of value projections from $\mathbf{X}$ and $\mathbf{U}$ respectively. While the softmax operation introduces query-key terms from both $\mathbf{X}, \mathbf{U}$ in both $\mathbf{Y}_x, \mathbf{Y}_u$, we are able to disentangle this influence in $\hat{\mathbf{Y}}_x, \hat{\mathbf{Y}}_u$ where $\mathbf{Y}$ lies in the convex combination of the two. By deriving bounds on the contribution from $\hat{\mathbf{Y}}_u$, we derive our controllability result. Intuitively, the reachable set exclusion condition in Equation 5 arises when the output representation $\hat{\mathbf{Y}}_x$ that occurs when only the imposed state $\mathbf{X}_0$ is fed into the transformer is too far away from the desired $\mathbf{Y}^*$ for the control tokens $\mathbf{U}$ to "steer" the output to $\mathbf{Y}^*$. The ability for the control input $\mathbf{U}$ to nullify the impact of $\hat{\mathbf{Y}}_x = \Xi(\mathbf{X}_0)$ on the output scales with the number of control input tokens k. A control input with many tokens can "dominate" the influence of $\mathbf{X}_0$ by re-allocating attention away from the component of the output $\hat{\mathbf{Y}}_x$ that arises from $\mathbf{X}_0$. A notable insight from the proof is that one may decompose the output of attention into a components that arise largely from different parts of the input. While there are cross terms in the attention matrix, these amount to only a positive scaling factor applied to the "independent" components like $\hat{\mathbf{Y}}_x$. Thus, we have an analytic bound on the reachable output set for self-attention (see further commentary in Section 6).

5. Experiments

To gain a practical, empirical understanding of the reachable set $\mathcal{R}_y^k(\mathbf{x}_0)$, we probe the existence of optimal prompts $\mathbf{u}^*$ across datasets $\mathcal{D}$ of initial state–desired output pairs $(\mathbf{x}_0, y^*)$. We scope our experiments to study immediate control (i.e., we check the LLM output after $|y^*|$ tokens are generated) where the control input $\mathbf{u}$ is prepended to the imposed state $\mathbf{x}_0$. Moreover, we focus on the case of controlling the LLM system to produce a single output token $y^* \in \mathcal{V}$ under some constraint $|u| \leq k$. This "single-step" control renders the problem of gauging reachability computationally tractable and is a fundamental step toward understanding the iterated dynamics of LLM systems in terms of reachability and controllability. We leave the exploration of reachability and controllability under an extended time horizon (e.g., chain-of-thought, chatbot dynamics, tool-wielding LLMs) and under the requirement of multi-token outputs $\mathbf{y}$ to future work.

5.1. Methods

We apply prompt optimization algorithms to establish the existence of optimal prompts $\mathbf{u}^*$ of length k that steer the LLM system from initial state $\mathbf{x}_0$ to output y for some dataset $\mathcal{D}$ of initial state-output pairs. In general, prompt optimization algorithms accept a token sequence and a loss function on said token sequence, along with a specification of which tokens are manipulable. The output of a prompt optimizer is a manipulated token sequence (i.e., optimized prompt) designed to minimize the loss. We apply two computational methods to generating optimal prompts: greedy back-generation (algorithm 2) and greedy coordinate gradient (GCG, invented in (Zou et al., 2023), algorithm 3). We found that greedy back-generation performed best for short prompts $k \leq 3$ tokens, while GCG was the best-performing algorithm for prompts of 4 or more tokens. To our knowledge, our greedy back-generation algorithm is novel. For brevity, we place the full description of the algorithms and our parameter values for the two algorithms in Appendix C, as the specifics of the algorithms are not the main contribution of this work.

We focus on understanding the content and structure of the reachable set of LLM system outputs $\mathcal{R}_y^k(\mathbf{x}_0)$, particularly under a constraint on the number of input tokens k. To determine which output tokens are reachable under varying input sequence lengths, we apply an incremental prompt lengthening procedure when searching for optimal prompts on some dataset $\mathcal{D}$.

5.2. Results

Our results revolve around the reachable set $\mathcal{R}_y^k(\mathbf{x}_0)$ for state sequences sampled from the Wikitext dataset. Results were computed for a panel of models, including Falcon-7b, Falcon-40b, and Llama-7b. Falcon-7b results are showcased in this section while additional plots and results for Falcon-40b and Llama-7b can be found in Section D. We applied the same Back-off Prompt strategy (Algorithm 1) to determine $k-\epsilon$ controllability for all experiments, varying the specifics of the dataset $\mathcal{D}$ for each experiment.

Algorithm 1 Back-off Prompt

Require: State-output token sequence $(\mathbf{x}_0, y)$; LLM system $\Sigma = (P_{LM}, \mathcal{V})$.
for $k = 1$ **to** 3 **do**
  $\mathbf{u}_k$ = Greedy Back Generate$(\mathbf{x}_0, y; \Sigma)$
  return $\mathbf{u}_k$ if it steers Σ from $\mathbf{x}_0 \to y$.
end for
for $k \in [4, 6, 8, 10]$ **do**
  $\mathbf{u}_k$ = Greedy Coordinate Gradient$(\mathbf{x}_0, y; \Sigma)$
  return $\mathbf{u}_k$ if it steers Σ from $\mathbf{x}_0 \to y$.
end for
return Failed to establish reachability. =0

"Ground truth" reachability: We established the reachability of the "ground truth" next token y proceeding state token sequence $\mathbf{x}_0$ in Wikitext. In our tests on a dataset of 5000 state-output sequences with states of length $8 - 32$ tokens, we found that the true next token y is reachable over 97% of the time across all models with a prompt of length $k \leq 10$ (Figure 2). Plots and supplementary figures for Falcon-40b and Llama-7b controllability w.r.t. ground truth Wikitext outputs can be found in Section D.1.

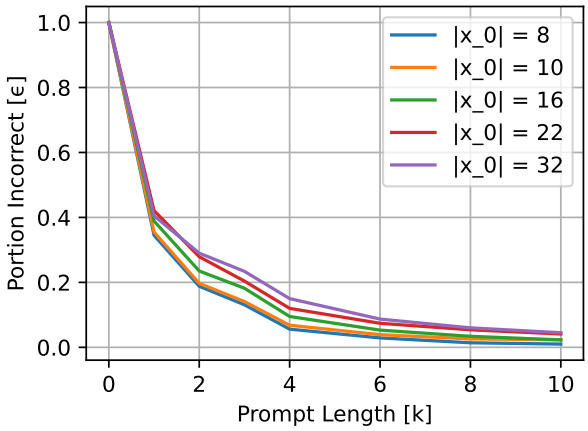

Figure 2. [Falcon-7b] $k - \epsilon$ values on initial state $\mathbf{x}_0$ and target output token y^* from Wikitext. 97.16% of the instances were solved with a prompt of length $k \leq 10$.

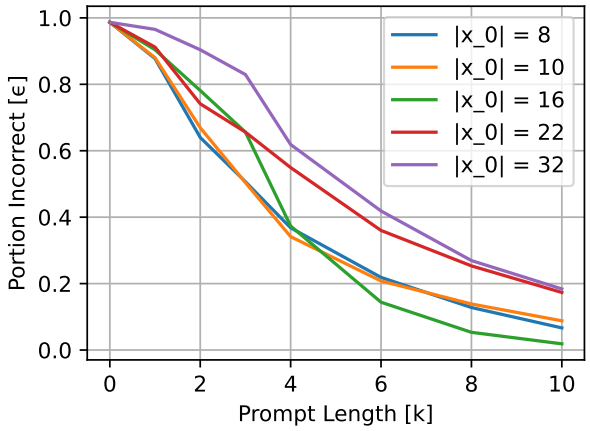

Figure 3. [Falcon-7b] $k - \epsilon$ values reaching the top 75 most likely outputs y^* for each $\mathbf{x}_0$ from Wikitext. The top 75 targets were reachable at least 89.39% of the time with a prompt of length $k \leq 10$.

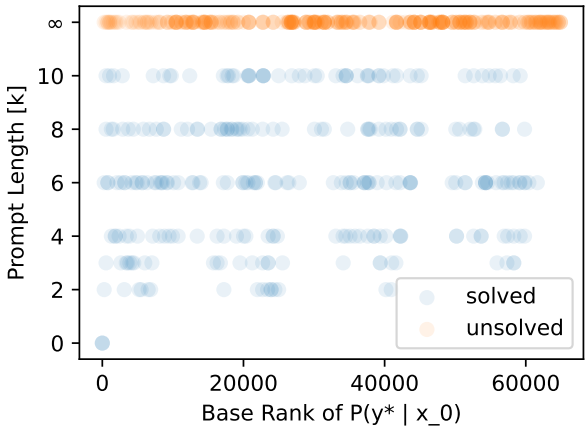

Figure 4. [Falcon-7b] Prior likelihood rank of target token y^* versus required prompt length to elicit y^*. Target tokens were sampled uniformly from the least to most likely token given $\mathbf{x}_0$ sampled from Wikitext.

Top-75 reachability: To explore the reachable set $R_y^k(\mathbf{x}_0)$ beyond the ground truth of Wikitext outputs, we generated a synthetic dataset of outputs by sampling 25 Wikitext sequences $\mathbf{x}_0$ and selecting the top 75 most likely next-tokens according to the model itself $P_{LM}(y|\mathbf{x}_0)$ as the target tokens (Figure 3). We found that the top 75 output tokens were reachable over 85% of the time for all models with control sequence length $k = 10$. Supplementary figures including results for Llama-7b and Falcon-40b on $k - \epsilon$ controllability with respect to the top 75 most likely output tokens can be found in Section D.2.

Uniformly sampled target outputs: To maximally push the bounds of the reachable set within our single output token scope, we created another synthetic dataset where the target output token y^* was sampled uniformly from the highest likelihood next token to the lowest likelihood token. Although the overall $k - \epsilon$ score was relatively poor (only 46.43% reachable with $k = 10$ for Falcon-7b), we were intrigued by the near-uniform relationship between prior token rank (based on $P_{LM}(y|\mathbf{x}_0)$) versus the required number of prompt tokens. Figure 4 plots the relationship between prior target token rank based on $P(y^*|\mathbf{x}_0)$ and the required prompt length k to elicit the prompt. While over half were unreachable, the remaining reachable tokens appear uniformly distributed in terms of required prompt length, regardless of rank. Supplementary figures analyzing the $k - \epsilon$ controllability of Falcon-7b with respect to uniformly sampled target outputs y can be found in Section D.3.

6. Discussion

We proposed a control theoretic framework for understanding language model prompting, orienting our investigation around the reachable set of outputs $\mathcal{R}_y^k(\mathbf{x}_0)$. We proved a bound on the reachable set of outputs for self-attention in terms of the singular values of its weight matrices, and we established fundamental results on the reachability of "correct" next tokens (according to Wikitext). We expanded the scope of this investigation by probing the reachability of tokens assigned high likelihood by the LLM itself, and tokens assigned minimal likelihood by the LLM itself.

Bounding the reachable set for self-attention is deeply related to the mechanism by which consistent representations are formed for multi-token generation. Steering a language model to generate a desired token sequence requires that the control input induce a token representation in the right-most token such that the next token prediction logits $P(\mathbf{y}|\mathbf{u}+\mathbf{x}_0)$ achieves a desired value. Moreover, generated tokens are fed back into the model, and their representations must be steered as well to control iterated generation. Self-attention is the primary mechanism by which the token representations exchange information, making the reachable set of output representations across multiple tokens in $\mathbf{X}_0$ for self-attention a fundamental part of LLM control theory.

Our empirical results suggest that there is far more to the reachability of a given output than just prior likelihood or the prior rank the LLM assigns to a given token. Although prompt optimization-based $k-\epsilon$ controllability experiments are only able to provide a lower bound on the content of the reachable set, the ability to frequently control even the *least*

likely token to being the *most likely* token with just a few input tokens is intriguing. We believe this result indicates the importance of further investigating the reachability and controllability of LLMs, particularly for developing capable and reliable LLM systems.

Our investigations provide an entry into the understanding of LLM controllability via prompts. However, a comprehensive understanding necessitates extending our exploration into diverse regimes. Exploring the controllability with longer prompts and longer questions (base token sequences) will be pivotal. Equally important is the study of diverse models to verify the generality of our findings. Moreover, the direct comparison of controllability scores of different model families is challenging since family uses a different tokenizer. The Llama family tokenizer, for instance, has a vocabulary of 30,000 tokens whereas the Falcon family has a vocabulary of 65,536 tokens. Further work is required to robustly compare controllability across models.

An intriguing observation from our study is the log-linear relationship between prompt length k and controllability fraction ϵ (see Figure 5 in Appendix D). While this is compelling within our studied domain, it raises the essential question: is this relationship robust outside our current explorative scope? Unearthing universal scaling laws in LLM controllability would not only inform practical control applications but also open the door for theoretical insight into the nature of LLM behavior.

The progress we have made, both in understanding the bounds on self-attention controllability and the empirical measures of $k - \epsilon$ LLM controllability, underscores the potential of this control theoretic framing for studying LLMs. Below is a non-exhaustive list of open problems in LLM control, all stemming from the framing in section A:

- **Control Properties of Chain-of-Thought:** Chain-of-Thought is a powerful technique where LLMs are allowed to generate intermediate tokens (i.e., "thoughts") between a question and an answer (Wei et al., 2023). The control properties (e.g., stability, reachability) of systems leveraging these techniques are of great interest for understanding and composing systems of LLMs in the real world.
- **Distributional Control:** To what extent can we control the output distribution of a language model $P_{LM}(\mathbf{y}|\mathbf{x}_0 + \mathbf{u})$ to a desired distribution $P^*(\mathbf{y})$?
- **Computational Cost of Control:** What are the performance characteristics of LLM control regularized by computational cost?
- **Learnability of Control:** To what extent can LLMs learn to control each other? Work such as (Zhou et al., 2023) showed that LLMs are capable of human-level prompt engineering, but it is unclear how well an LLM can learn to control another when explicitly optimized on the objective of LLM control.
- **Controllable Subspaces:** In the control of linear dynamical systems, it is known that uncontrollable systems are often coordinate transformable into a representation where a subset of the coordinates are controllable and a subset are uncontrollable (Sontag, 2013). We have shown that controllable and uncontrollable components naturally emerge for self-attention heads in section 4 – can this be generalized to transformer blocks with nonlinearities and residual streams?
- **Composable LLM Systems:** One of the greatest boons of control theory is the ability to compose control modules and subsystems into an interpretable, predictable, and effective whole (Lian et al., 2002). The composition of LLM systems (potentially with non-LLM control modules) is an exciting avenue for scaling super intelligent systems.

The originality of our approach lies in the fusion of control theory with the domain of LLMs, an intersection scarcely explored in current research. This novel perspective not only enriches our theoretical understanding of LLM behavior but also opens new pathways for practical applications. By framing LLM prompting within the control theoretic paradigm, we bridge a gap between abstract mathematical concepts and tangible LLM functionalities. This melding of fields is not just an academic exercise; it holds potential for significant advancements in areas such as natural language generation, conversational AI, and even in developing more interpretable LLMs.

Practically, our findings lay the groundwork for more effective and efficient prompt engineering. The ability to control even the least likely tokens illuminates untapped capabilities within LLMs, hinting at a much broader spectrum of application than previously recognized. Such insights could lead to the development of more nuanced and sophisticated LLM systems, capable of handling complex tasks with greater precision and adaptability. Ultimately, the practical significance of our work lies in its potential to transform how we interact with, understand, and utilize LLMs in both research and real-world applications.

Impact statement

This paper introduces foundational work aimed at enhancing our understanding and control of generative language models (LLMs) as they become integral to crucial societal functions. The increasing integration of generative AI into critical infrastructures — such as healthcare data analysis, insurance and financial data processing, and emergency response systems — underscores the urgency for a sophisticated control theory. Drawing on the principles of control theory, which have historically ensured the dependability of machines in life-or-death scenarios (e.g., in cruise control and aircraft navigation systems), our goal is to extend these guarantees to LLM-based applications. By doing so, we aim to make these advanced AI systems as trustworthy and robust as their electro-mechanical counterparts, thereby securing their role in supporting and safeguarding society.

Code availability

All code used to produce the experimental results is provided with the submission.

References

Almazrouei, E., Alobeidli, H., Alshamsi, A., Cappelli, A., Cojocaru, R., Debbah, M., Goffinet, E., Heslow, D., Launay, J., Malartic, Q., Noune, B., Pannier, B., and Penedo, G. Falcon-40B: an open large language model with state-of-the-art performance. 2023.

Aniţa, S., Arnăutu, V., Capasso, V., and Capasso, V. *An introduction to optimal control problems in life sciences and economics: From mathematical models to numerical simulation with MATLAB®*, volume 2. Springer, 2011.

Bahdanau, D., Cho, K., and Bengio, Y. Neural machine translation by jointly learning to align and translate, 2016.

Bai, Y., Jones, A., Ndousse, K., Askell, A., Chen, A., DasSarma, N., Drain, D., Fort, S., Ganguli, D., Henighan, T., et al. Training a helpful and harmless assistant with reinforcement learning from human feedback. *arXiv preprint arXiv:2204.05862*, 2022.

Bricken, T., Templeton, A., Batson, J., Chen, B., Jermyn, A., Conerly, T., Turner, N., Anil, C., Denison, C., Askell, A., Lasenby, R., Wu, Y., Kravec, S., Schiefer, N., Maxwell, T., Joseph, N., Hatfield-Dodds, Z., Tamkin, A., Nguyen, K., McLean, B., Burke, J. E., Hume, T., Carter, S., Henighan, T., and Olah, C. Towards monosemanticity: Decomposing language models with dictionary learning. *Transformer Circuits Thread*, 2023. https://transformer-circuits.pub/2023/monosemantic-features/index.html.

Brown, T., Mann, B., Ryder, N., Subbiah, M., Kaplan, J. D., Dhariwal, P., Neelakantan, A., Shyam, P., Sastry, G., Askell, A., Agarwal, S., Herbert-Voss, A., Krueger, G., Henighan, T., Child, R., Ramesh, A., Ziegler, D., Wu, J., Winter, C., Hesse, C., Chen, M., Sigler, E., Litwin, M., Gray, S., Chess, B., Clark, J., Berner, C., McCandlish, S., Radford, A., Sutskever, I., and Amodei, D. Language models are few-shot learners. In Larochelle, H., Ranzato, M., Hadsell, R., Balcan, M., and Lin, H. (eds.), *Advances in Neural Information Processing Systems*, volume 33, pp. 1877–1901. Curran Associates, Inc., 2020. URL https://proceedings.neurips.cc/paper_files/paper/2020/file/1457c0d6bfcb4967418bfb8ac142f64a-Paper.pdf.

Bubeck, S., Chandrasekaran, V., Eldan, R., Gehrke, J., Horvitz, E., Kamar, E., Lee, P., Lee, Y. T., Li, Y., Lundberg, S., Nori, H., Palangi, H., Ribeiro, M. T., and Zhang, Y. Sparks of artificial general intelligence: Early experiments with gpt-4, 2023.

Calafiore, G. C. and El Ghaoui, L. *Optimization models*. Cambridge university press, 2014.

Chefer, H., Gur, S., and Wolf, L. Transformer interpretability beyond attention visualization, 2021.

Conmy, A., Mavor-Parker, A. N., Lynch, A., Heimersheim, S., and Garriga-Alonso, A. Towards automated circuit discovery for mechanistic interpretability, 2023.

Goodfellow, I. J., Shlens, J., and Szegedy, C. Explaining and harnessing adversarial examples, 2015.

Guo, C., Sablayrolles, A., Jégou, H., and Kiela, D. Gradient-based adversarial attacks against text transformers, 2021.

Hagendorff, T. Machine psychology: Investigating emergent capabilities and behavior in large language models using psychological methods, 2023.

Jiang, Z., Xu, F. F., Araki, J., and Neubig, G. How can we know what language models know?, 2020.

Kalman, R. E., Falb, P. L., and Arbib, M. A. *Topics in mathematical system theory*, volume 33. McGraw-Hill New York, 1969.

Lewis, P., Perez, E., Piktus, A., Petroni, F., Karpukhin, V., Goyal, N., Küttler, H., Lewis, M., Yih, W.-t., Rocktäschel, T., et al. Retrieval-augmented generation for knowledge-intensive nlp tasks. *Advances in Neural Information Processing Systems*, 33:9459–9474, 2020.

Lian, F.-L., Moyne, J., and Tilbury, D. Network design consideration for distributed control systems. *IEEE transactions on control systems technology*, 10(2):297–307, 2002.

Merity, S., Xiong, C., Bradbury, J., and Socher, R. Pointer sentinel mixture models, 2016.

Min, B., Ross, H., Sulem, E., Veyseh, A. P. B., Nguyen, T. H., Sainz, O., Agirre, E., Heintz, I., and Roth, D. Recent advances in natural language processing via large pre-trained language models: A survey. *ACM Computing Surveys*, 56(2):1–40, 2023.

Noever, D. and McKee, F. Numeracy from literacy: Data science as an emergent skill from large language models, 2023.

Ogata, K. *Modern control engineering fifth edition*. 2010.

OpenAI, Nov 2022. URL https://openai.com/blog/chatgpt.

OpenAI. Gpt-4 technical report, 2023.

Patil, S. G., Zhang, T., Wang, X., and Gonzalez, J. E. Gorilla: Large language model connected with massive apis, 2023.

Petroni, F., Rocktäschel, T., Lewis, P. S. H., Bakhtin, A., Wu, Y., Miller, A. H., and Riedel, S. Language models as knowledge bases? *CoRR*, abs/1909.01066, 2019. URL http://arxiv.org/abs/1909.01066.

Radford, A., Wu, J., Child, R., Luan, D., Amodei, D., Sutskever, I., et al. Language models are unsupervised multitask learners. *OpenAI blog*, 1(8):9, 2019.

Reynolds, L. and McDonell, K. Prompt programming for large language models: Beyond the few-shot paradigm, 2021.

Roy, S., Wan, Y., and Saberi, A. A network control theory approach to virus spread mitigation. In *2009 IEEE Conference on Technologies for Homeland Security*, pp. 599–606, 2009. doi: 10.1109/THS.2009.5168092.

Rozière, B., Gehring, J., Gloeckle, F., Sootla, S., Gat, I., Tan, X. E., Adi, Y., Liu, J., Remez, T., Rapin, J., Kozhevnikov, A., Evtimov, I., Bitton, J., Bhatt, M., Ferrer, C. C., Grattafiori, A., Xiong, W., Défossez, A., Copet, J., Azhar, F., Touvron, H., Martin, L., Usunier, N., Scialom, T., and Synnaeve, G. Code llama: Open foundation models for code, 2023.

Shi, W., Han, X., Gonen, H., Holtzman, A., Tsvetkov, Y., and Zettlemoyer, L. Toward human readable prompt tuning: Kubrick's the shining is a good movie, and a good prompt too?, 2022.

Shin, T., Razeghi, Y., au2, R. L. L. I., Wallace, E., and Singh, S. Autoprompt: Eliciting knowledge from language models with automatically generated prompts, 2020.

Sivaramakrishnan, K., Sivaramakrishnan, V., and Oishi, M. M. K. Stochastic reachability of discrete-time stochastic systems via probability measures, 2023.

Soatto, S., Tabuada, P., Chaudhari, P., and Liu, T. Y. Taming ai bots: Controllability of neural states in large language models, 2023.

Sontag, E. D. *Mathematical control theory: deterministic finite dimensional systems*, volume 6. Springer Science & Business Media, 2013.

Taylor, W. L. "cloze procedure": A new tool for measuring readability. *Journalism Quarterly*, 30(4):415–433, 1953. doi: 10.1177/107769905303000401. URL https://doi.org/10.1177/107769905303000401.

Touvron, H., Lavril, T., Izacard, G., Martinet, X., Lachaux, M.-A., Lacroix, T., Rozière, B., Goyal, N., Hambro, E., Azhar, F., Rodriguez, A., Joulin, A., Grave, E., and Lample, G. Llama: Open and efficient foundation language models, 2023.

Vaswani, A., Shazeer, N., Parmar, N., Uszkoreit, J., Jones, L., Gomez, A. N., Kaiser, Ł., and Polosukhin, I. Attention is all you need. *Advances in neural information processing systems*, 30, 2017.

Wang, L., Lyu, C., Ji, T., Zhang, Z., Yu, D., Shi, S., and Tu, Z. Document-level machine translation with large language models. *arXiv preprint arXiv:2304.02210*, 2023a.

Wang, Z., Xie, Q., Ding, Z., Feng, Y., and Xia, R. Is chatgpt a good sentiment analyzer? a preliminary study. *arXiv preprint arXiv:2304.04339*, 2023b.

Wei, J., Tay, Y., Bommasani, R., Raffel, C., Zoph, B., Borgeaud, S., Yogatama, D., Bosma, M., Zhou, D., Metzler, D., Chi, E. H., Hashimoto, T., Vinyals, O., Liang, P., Dean, J., and Fedus, W. Emergent abilities of large language models, 2022.

Wei, J., Wang, X., Schuurmans, D., Bosma, M., Ichter, B., Xia, F., Chi, E., Le, Q., and Zhou, D. Chain-of-thought prompting elicits reasoning in large language models, 2023.

Wen, Y., Jain, N., Kirchenbauer, J., Goldblum, M., Geiping, J., and Goldstein, T. Hard prompts made easy: Gradient-based discrete optimization for prompt tuning and discovery, 2023.

Weston, J., Bordes, A., Chopra, S., and Mikolov, T. Towards ai-complete question answering: A set of prerequisite toy tasks. In Bengio, Y. and LeCun, Y. (eds.), *4th International Conference on Learning Representations, ICLR 2016, San Juan, Puerto Rico, May 2-4, 2016, Conference Track Proceedings*, 2016. URL http://arxiv.org/abs/1502.05698.

Yi, T.-M., Huang, Y., Simon, M. I., and Doyle, J. Robust perfect adaptation in bacterial chemotaxis through integral feedback control. *Proceedings of the National Academy of Sciences*, 97(9):4649–4653, 2000.

Zhang, H., Song, H., Li, S., Zhou, M., and Song, D. A survey of controllable text generation using transformer-based pre-trained language models. *CoRR*, abs/2201.05337, 2022. URL https://arxiv.org/abs/2201.05337.

Zhou, Y., Muresanu, A. I., Han, Z., Paster, K., Pitis, S., Chan, H., and Ba, J. Large language models are human-level prompt engineers, 2023.

Zou, A., Wang, Z., Kolter, J. Z., and Fredrikson, M. Universal and transferable adversarial attacks on aligned language models, 2023.

A. Abstract Systems and Control Theory Background

This section aims to provide an overview of fundamental control-theoretic concepts from an abstract, set-theoretic perspective. We primarily draw from (Sontag, 2013; Kalman et al., 1969), and (Ogata, 2010).

Diverse definitions of "system" or "machine" exist in the literature, all representing the same core concept but varying in mathematical details. We offer the following high-level definition based on (Sontag, 2013):

Definition A.1 (System)**.** A "system" or "machine" $\Sigma = (\mathcal{T}, \mathcal{X}, \mathcal{U}, \phi)$ consists of:

- $\mathcal{T}$: The **time set** along which system state evolves.
- $\mathcal{X}$: The **state space**.
- $\mathcal{U}$: The **input space**.
- $\phi : \mathcal{X} \times \mathcal{U} \times \mathcal{T}^2 \to \mathcal{X}$: The **transition map**.

A system may also be equipped with an output space and readout map $(\mathcal{Y}, h)$:

- $\mathcal{Y}$: The **output space**.
- $h : \mathcal{X} \times \mathcal{U} \times \mathcal{T} \to \mathcal{Y}$: The **readout map**.

In other words, at time $t \in \mathcal{T}$, the system's state takes on values $x \in \mathcal{X}$, and the control input takes values $u \in \mathcal{U}$. The system evolves over time with the transition map $\phi(x, u, t, t')$ that returns the new state value $x' \in \mathcal{X}$ at time $t' > t$. A system can also have a readout map $h(x, u, t)$ that produces the output value $y \in \mathcal{Y}$ given the current time, state, and input value. An input $u \in \mathcal{U}$ defined over interval $[t, t']$ may be said to *steer the system* $\Sigma = (\mathcal{T}, \mathcal{X}, \mathcal{U}, \phi)$ from state x_0 to state x' if $x' = \phi(x_0, u, t, t')$. A wide variety of systems are expressible within this framework. E.g., we obtain discrete-time dynamical systems for $\mathcal{T} = \mathbb{Z}^+$. Continuous-time dynamical systems emerge for $\mathcal{T} = \mathbb{R}^+$.

Note that we assume that the system Σ is time-invariant; its dynamics ϕ do not change as a function of time. This assumption is widely applicable and is often made in the literature (Kalman et al., 1969; Ogata, 2010; Sontag, 2013) to simplify definitions and discussions of systems.

Reachability is a core control theory concept and central to defining controllability. At their core, definitions of reachability revolve around the existence of control inputs $u \in \mathcal{U}$ that steer the system from a starting state $x_0 \in \mathcal{X}$ to some desired state(s). Following from (Kalman et al., 1969; Sontag, 2013), we define state reachability as:

Definition A.2 (State Reachability)**.** State $x \in \mathcal{X}$ is reachable from initial state $x_0 \in \mathcal{X}$ for system $\Sigma = (\mathcal{T}, \mathcal{X}, \mathcal{U}, \phi)$ iff there exists some time T and control input $u^* \in \mathcal{U}$ such that u^* steers the system from state x_0 to state x at time T.

We may use this definition of state reachability to define the reachable state set for some initial state $x_0 \in \mathcal{X}$:

Definition A.3 (Reachable State Set)**.** The reachable state set from initial state $x_0 \in \mathcal{X}$ for system $\Sigma = (\mathcal{T}, \mathcal{X}, \mathcal{U}, \phi)$ is denoted $\mathcal{R}(x_0) \subseteq \mathcal{X}$ and consists of all reachable states $x \in \mathcal{X}$ from initial state x_0 (cf. Definition A.2).

For systems with readout maps h, notions of *output reachability* arise naturally. Note that state reachability is neither necessary nor sufficient to guarantee output reachability.

Definition A.4 (Output Reachability)**.** Output $y \in \mathcal{Y}$ is reachable from initial state $x_0 \in \mathcal{X}$ for system $\Sigma = (\mathcal{T}, \mathcal{X}, \mathcal{U}, \phi, \mathcal{Y}, h)$ iff there exists some time T and control input $u^* \in \mathcal{U}$ such that u^* steers the system from state x_0 to output y in time T.

Definition A.5 (Reachable Output Set)**.** The reachable output set from initial state $x_0 \in \mathcal{X}$ for system $\Sigma = (\mathcal{T}, \mathcal{X}, \mathcal{U}, \phi, \mathcal{Y}, h)$ is denoted $\mathcal{R}_y(x_0)$ and consists of all reachable outputs $y \in \mathcal{Y}$ from initial state x_0 (cf. Definition A.4).

A system is controllable when the reachable set extends to the entire state space. Practically speaking, this implies that one can steer the system from any initial state to any desired state.

Definition A.6 (State Controllability)**.** System $\Sigma = (\mathcal{T}, \mathcal{X}, \mathcal{U}, \phi)$ is state controllable iff, for every initial state $x_0 \in \mathcal{X}$, the reachable set $\mathcal{R}(x_0) = \mathcal{X}$.

Definition A.7 (Output Controllability)**.** System $\Sigma = (\mathcal{T}, \mathcal{X}, \mathcal{U}, \phi, \mathcal{Y}, h)$ is output controllable iff, for every initial state $x_0 \in \mathcal{X}$, the reachable output set $\mathcal{R}_y(x_0) = \mathcal{Y}$.

A range of fruitful questions stem from these definitions: if there is a cost associated with control inputs $u \in \mathcal{U}$ (e.g., power constraints, length constraints), what is the minimum cost of control? What is the minimum time required to get from the initial state to the desired final state or output? If the system is not completely controllable, under what conditions is it controllable? Under which readout maps is a system output controllable?

B. Proof of Self-Attention Controllability Theorem 4.2

Note: Key terms for the proof are introduced in Section 4 surrounding Theorem 4.2. Specifically, the definition of self-attention mechanism Ξ, the control problem setup, and the reachable set $\mathcal{R}_y^k(\mathbf{X}_0)$ are required background for this proof.

Proof. For each token representation matrix $\mathbf{Q}, \mathbf{K}, \mathbf{V} \in \mathbb{R}^{(k+M)\times \cdot}$, we denote the first k rows corresponding to $\mathbf{U}$ using u as a subscript, like $\mathbf{Q}_u$. The remaining M rows corresponding to $\mathbf{X}_0$ are denoted with subscript x like $\mathbf{Q}_x$.

Let $\mathbf{A}$ be the exponentiated query-key outer product matrix with the following block structure:

$$\mathbf{A} = \exp\left(\frac{\mathbf{Q}\,\mathbf{K}^\top}{\sqrt{d_k}}\right) = \exp\left(\begin{bmatrix} \mathbf{Q_u}\mathbf{K_u}^\top & \mathbf{Q_u}\mathbf{K_x}^\top \\ \mathbf{Q_x}\mathbf{K_u}^\top & \mathbf{Q_x}\mathbf{K_x}^\top \end{bmatrix} \tfrac{1}{\sqrt{d_k}}\right) = \begin{bmatrix} \mathbf{A}_{uu} & \mathbf{A}_{ux} \\ \mathbf{A}_{xu} & \mathbf{A}_{xx} \end{bmatrix} \tag{8}$$

We apply a similar quadrant decomposition to $\mathbb{D}$, defined initially in Equation 4.

$$\mathbb{D} = \operatorname{diag}\left(\exp\left(\frac{\mathbf{Q}\mathbf{K}^\top}{\sqrt{d_k}}\right)\mathbf{1}_{N\times 1}\right) = \begin{bmatrix} \mathbb{D}_u & \mathbf{0} \\ \mathbf{0} & \mathbb{D}_x \end{bmatrix} \tag{9}$$

where the quadrant demarcations in $\mathbb{D}$ follow from Equation 8.

We may now express the self-attention mechanism output representations $\mathbf{Y}$ as

$$\mathbf{Y} = \mathbb{D}_x^{-1}\mathbf{A}_{xu}\mathbf{V}_u + \mathbb{D}_x^{-1}\mathbf{A}_{xx}\mathbf{V}_x \tag{10}$$

We begin by stating the equality between the desired output $\mathbf{Y}^*$ and the true system output from Equation 10. The final bound in Equation 5 of Theorem 4.2 is derived by isolating terms depending on control input $\mathbf{U}$, bounding them, and expressing that bound as a condition for achieving equality between the desired output $\mathbf{Y}^*$ and the true system output.

$$\mathbf{Y}^* = \underbrace{\mathbb{D}_x^{-1}\mathbf{A}_{xu}\mathbf{V}_u}_{\triangleq \mathbf{Y}_u} + \underbrace{\mathbb{D}_x^{-1}\mathbf{A}_{xx}\mathbf{V}_x}_{\triangleq \mathbf{Y}_x} \tag{11}$$

$$\implies \mathbf{Y}_u = \mathbf{Y}^* - \mathbf{Y}_x \tag{12}$$

We may immediately bound the magnitude of the rows of $\mathbf{Y}_u$ as the matrix $\mathbb{D}_x^{-1}\mathbf{A}_{x_u}$ has rows that sum to less than 1 (it represents one quadrant of the row-wise softmaxed attention map, which has rows that sum to 1 by construction). Therefore, each row $\mathbf{y}_u^i$ of $\mathbf{Y}_u$ lies within the convex hull defined by the row vectors $\mathbf{v}_u^i$ of $\mathbf{V}_u$. Recalling Definition 4.1, $\mathbf{V}_u = \mathbf{U}\mathbf{W_v}$. Let $\Omega_u = \max_j \|\mathbf{u}^j\|$ for rows $\mathbf{u}^j$ of $\mathbf{U}$, we can bound the norm of each $\mathbf{v}_u^i$ in $\mathbf{V}_u$ with the maximum singular value of parameter matrix $\mathbf{W}_v$, denoted σ_q. Refer to Chapter 5 of (Calafiore & El Ghaoui, 2014) for an overview of singular values. Thus we may bound each $\|\mathbf{v}_u^i\| \leq \Omega_u\sigma_q$. By the properties of convex hulls, each row of $\mathbf{Y}_u$ must inherit this upper bound on magnitude to retain feasibility.

$$\|\mathbf{y}_u^i\| < \Omega_u\sigma_q \tag{13}$$

Refer to Chapter 8 of (Calafiore & El Ghaoui, 2014) for a detailed explanation of convex hulls and their properties.

While $\mathbf{Y}_x$ in Equation 11 may appear to depend only on imposed $\mathbf{X}_0$, the denominator term $\mathbb{D}_x^{-1}$ contains influences from $\mathbb{U}$. Let us split the denominator term $\mathbb{D}_x = \hat{\mathbf{D}}_{xx} + \hat{\mathbf{D}}_{xu}$ where $\hat{\mathbf{D}}_{xx}$ depends solely on the imposed input $\mathbb{X}_0$. $\hat{\mathbf{D}}_{xx}$ is definedin Equation 6. Let $\hat{\mathbf{D}}_{xu}$ be defined as:

$$\hat{\mathbf{D}}_{xu} = \operatorname{diag}\left(\exp\left(\frac{\mathbf{Q_x}\mathbf{K_u}^\top}{\sqrt{d_k}}\right)\mathbf{1}_{k\times 1}\right) \tag{14}$$

Recall Equation 7, which defines $\hat{\mathbf{Y}}_x$, the output of Ξ if only $\mathbf{X}_0$ is input. Let us express the condition in Equation 11 using $\hat{\mathbf{Y}}_x$ to disentangle the influence of the control input:

$$\mathbf{Y}_u = \mathbf{Y}^* - (\hat{\mathbf{D}}_{xu} + \hat{\mathbf{D}}_{xx})^{-1}\hat{\mathbf{D}}_{xx}\hat{\mathbf{Y}}_x \tag{15}$$

Observe that the rows of $\mathbf{Y}_x$ and $\hat{\mathbf{Y}}_x$ are positively scaled versions of each other because the denominator matrices are all positive and diagonal. Applying the bound in Equation 13 using row-wise notation,

$$\|\mathbf{y}^{*i} - \frac{\hat{D}^i_{xx}}{\hat{D}^i_{xx} + \hat{D}^i_{xu}}\hat{\mathbf{y}}^i_x\| \leq \sigma_q \Omega_u \tag{16}$$

Using the same singular values reasoning as in Equation 13 to bound the unknown denominator term $\hat{D}^i_{xu}$, which is the only term still dependent on the control input U.

$$\hat{D}^i_{xu} \leq k \exp\left(\frac{\Omega_x \sigma_q \sigma_k \Omega_u}{\sqrt{d_k}}\right) \tag{17}$$

Achieving this minimum value will minimize the value of $\mathbf{y}^i_x$ by maximally scaling down $\hat{\mathbf{y}}^i_x$. The maximum value for $\mathbf{y}^i_x$ arises when $\hat{D}^i_{xu}$ is minimized (e.g., to zero) resulting in $\mathbf{y}^i_x = \hat{\mathbf{y}}^i_x$.

Therefore, the the value of $\mathbf{y}^i_x$ is constrained linear scalings between this minimum and this maximum. If every scaling violates the inequality in Equation 16, then the system is strictly controllable.

Therefore, if $\langle \mathbf{y}^{*i}, \hat{\mathbf{y}}^i_x \rangle \leq 0$ for some row i following inequality is met, the output Y^* is **strictly unreachable** under imposed input representations $\mathbf{X}_0$ and control input $\mathbf{U}$:

$$\|\mathbf{y}^{*i} - \frac{\hat{D}^i_{xx}}{\hat{D}^i_{xx} + k \exp\left(\frac{\Omega_x \sigma_q \sigma_k \Omega_u}{\sqrt{d_k}}\right)}\hat{\mathbf{y}}^i_x\| \leq \sigma_q \Omega_u \tag{18}$$

□

C. Prompt Optimization Algorithms

Greedy Back-Generation: While testing all prompts in $\mathcal{V}^k$ is intractable for $k > 1$, it takes only $|\mathcal{V}|$ forward passes of the network to compute the loss on y induced by all possible *single token* prompts $u \in \mathcal{V}$. Our Greedy Back Generation algorithm leverages this fact to generate prompts $u \in \mathcal{V}^k$ one token at a time, working backward sampling the ith greedy-optimal single token extension $u' = \arg\max_{u'} P_{LM}(y|u' + u + x)$ of the current prompt $u \in \mathcal{V}^{i-1}$.

This method is optimal for $k = 1$ prompt token $u^* \in \mathcal{V}$ and generally outperforms GCG for short prompts of length $k \leq 3$. Computing 1 additional prompt token takes roughly 1-4 minute when using an NVIDIA A100-80GB GPU with a 7 billion parameter model and 5-20 minutes on 2 NVIDIA A100-80GB GPUs with a 40 billion parameter model.

Greedy Coordinate Gradient (GCG): The Greedy Coordinate Gradient algorithm, presented by (Zou et al., 2023) building off the work of (Shin et al., 2020), is the state-of-the-art method for optimizing prompts. Starting with a random prompt of length k, the algorithm generates a batch of alternative prompts. Each member of the batch swaps a random token in the current prompt with a promising alternate token. The value metric for a swap is given by a first order approximation of the change in loss $\mathcal{L} = \text{CELoss}(y, P_{LM}(y|u + x))$ with the embedding of each token in u.

This method outperforms all other methods we tested for prompts of length $k > 3$. We use a batch size $B = 768$, sampled from the top $k_{sub} = 128$ token replacements at each index, and iterate for $T = 34$ iterations. For each instance, this optimization took roughly 2 minutes for the 7 billion parameter models on a single A100-80GB GPU and 4-8 minutes for the 40 billion parameter model on 4 A100-80GB GPU.

Algorithm 2 Greedy Token-Wise Prompt Generation

Require: A causal LLM P_{LM} with vocabulary $\mathcal{V}$, a set of base tokens $x \in \mathcal{V}^n$, a desired final token $y \in \mathcal{V}$, and a desired number of prompt tokens k.
Ensure: *Magic words* u^* of length k.
Initialize u^* to be empty.
for $i = 1$ **to** k **do**
  for all $u' \in \mathcal{V}$ **do**
    compute $P_{LM}(y|u' + u^* + x)$
  end for
  Select the u' that maximizes the probability of y given $u' + u^* + x$. Prepend u' to u^*
end for
return u^* =0

Algorithm 3 Greedy Coordinate Gradient

Require: A causal LLM P_{LM} that accepts token strings from a vocabulary $\mathcal{X}$, an embedding dictionary $\mathbf{e}$, embeddings $\mathbf{e}_i^*$ corresponding to each token i of u^*, a set of base tokens $x_{1:n}$, a desired number of prompt tokens k, iterations T, k_{sub}, and batch size B.
Ensure: *Magic words* u^* of length k.
Initialize u^* to be random tokens from vocabulary.
for $iteration = 1$ **to** T **do**
  for $i = 1$ **to** k **do**
    $\mathcal{X}_i = \text{Top-}k_{sub}\ (\mathbf{e}^T \nabla_{\mathbf{e}_i^*} P_{LM}(x_n|u^* + x_{1:n-1}))$
  end for
  for $b = 1$ **to** B **do**
    $i = \text{randint}([1, \ldots, k])$
    $j = \text{randint}([1, \ldots, k_{sub}])$
    $\tilde{u}_b^*[i] = \mathcal{X}_i[j]$
  end for
  $u^* = \tilde{u}_{b^*}^*$, where $b^* = \text{argmax}_b(P_{LM}(x_n|u^* + x_{1:n-1}))$
end for
return u^* =0

D. Supplementary Figures: Optimal Control Prompts

D.1. "Ground Truth" Controllability Results

This subsection includes supplementary figures for the controllability of Llama-7b, Falcon-7b, and Falcon-40b "ground truth" target outputs from Wikitext. For each initial state sequence $\mathbf{x}_0$, the target output y is the token immediately following $\mathbf{x}_0$ in Wikitext. We measured the $k - \epsilon$ controllability of each of the 7 billion parameter models with a dataset of 5000 state-output pairs while we used a dataset of 500 state-output pairs for Falcon-40b.

Figure 5 shows each model's log-spaced $k - \epsilon$ curves on the Wikitext dataset, revealing a log-linear relationship between maximum prompt length k and the fraction of uncontrollable initial state-target output pairs $(\mathbf{x}_0, y)$. We visualize the relationship between prompt length and the prior cross-entropy loss of each LLM on predicting the target output y given the state sequence $\mathbf{x}_0$ (i.e., $-\log P_{LM}(y|\mathbf{x}_0)$ in Figure 6 where we find it difficult to predict the required prompt length from the base loss.

Finally, Figure 7 shows a histogram of the tokens in the optimized prompts generated in the ground truth $k - \epsilon$ controllability experiments on Wikitext.

D.2. Top-75 Wikitext Controllability Results

This subsection includes supplementary figures for the controllability of Llama-7b, Falcon-7b, and Falcon-40b on the Wikitext dataset where the target output token y for a given initial state token sequence $\mathbf{x}_0$ is sampled uniformly from the top 75 highest-probability tokens as determined by the language model itself $P_{LM}(y|\mathbf{x}_0)$. Specifically, the dataset $\mathcal{D}$ consists of

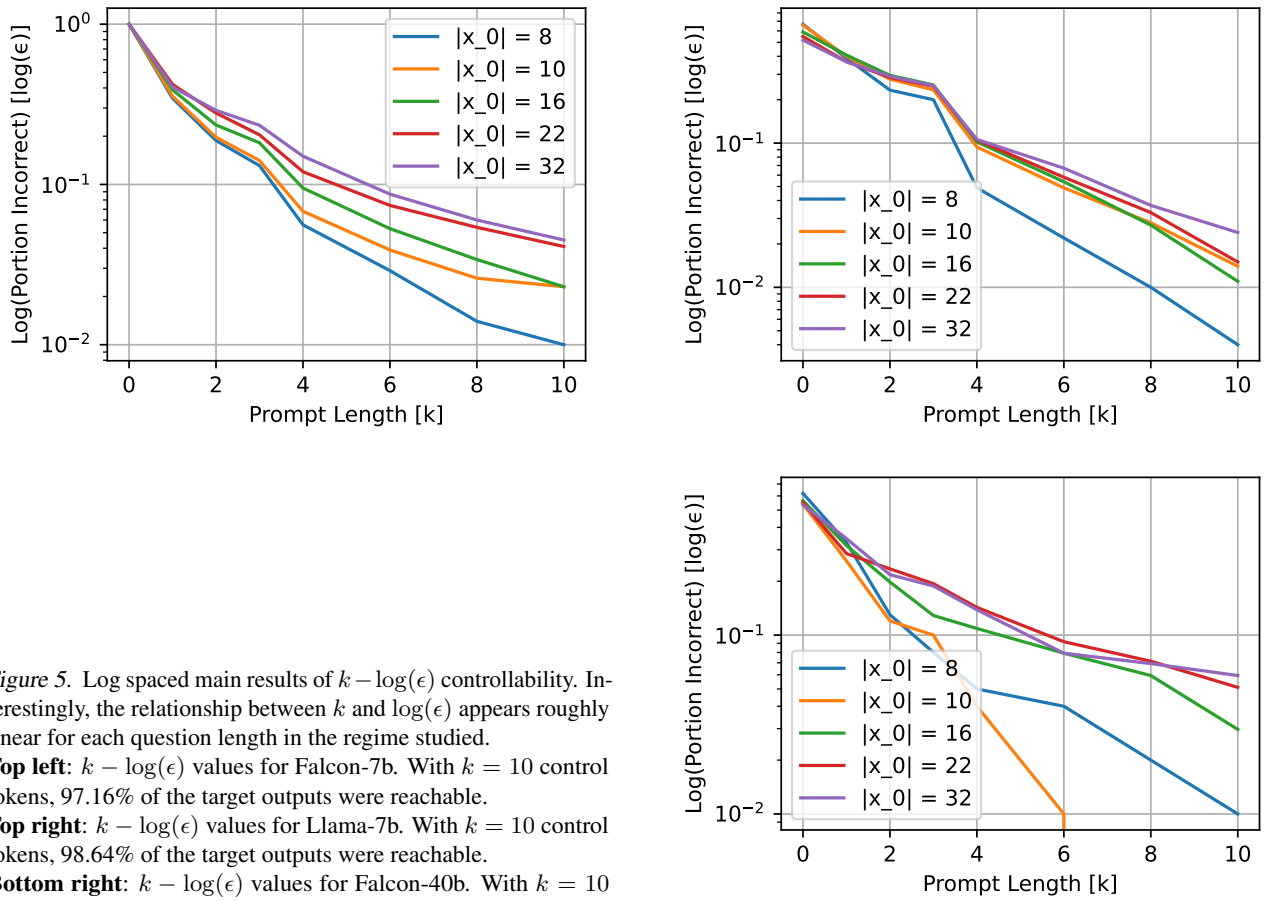

Figure 5. Log spaced main results of $k - \log(\epsilon)$ controllability. Interestingly, the relationship between k and $\log(\epsilon)$ appears roughly linear for each question length in the regime studied.
Top left: $k - \log(\epsilon)$ values for Falcon-7b. With $k = 10$ control tokens, 97.16% of the target outputs were reachable.
Top right: $k - \log(\epsilon)$ values for Llama-7b. With $k = 10$ control tokens, 98.64% of the target outputs were reachable.
Bottom right: $k - \log(\epsilon)$ values for Falcon-40b. With $k = 10$ control tokens, 97.00% of the target outputs were reachable.

25 unique initial state token sequences $\mathbf{x}_0$ sampled from Wikitext, each replicated 75 times for the top 75 most probable subsequent tokens $y \sim P(y|\mathbf{x}_0)$. This procedure yielded a dataset of 1875 initial state-target output pairs $(\mathbf{x}_0, y)$ for the 7 billion parameter models. Due to the computational requirements for the 40 billion parameter model, the number of unique initial state token sequences was decreased to 10, resulting in a dataset of 750 initial state-target output pairs. The $k - \epsilon$ plots for each model are shown in Figure 8. On average, across the 3 models, the top 75 outputs were reachable 86.865% of the time with $k \leq 10$ prompt tokens. Similar log-linear trends were observed in the $k - \epsilon$ plot. Figure 9 shows the relationship between base loss and required prompt length, revealing a more dramatic "exclusion zone" in the top left, similar to main "ground truth" results in Figure 6. Finally, Figure 10 plots a histogram of the 40 most common tokens observed in the optimized control input prompts from the top-75 experiments.

D.3. Uniformly Sampled Output Token Results

This section contains supplementary figures for $k - \epsilon$ controllability experiments on a synthetic dataset $\mathcal{D} = \{(\mathbf{x}_0, y)\}$ where $\mathbf{x}_0$ are sampled from the Wikitext dataset and y is sampled uniformly from the vocabulary. The uniform target output dataset $\mathcal{D}$ consists of 616 state-output pairs. Due to computational constraints, $k - \epsilon$ controllability was only measured for Falcon-7b. Overall, only 46.42% of the target outputs were reachable with $k = 10$ prompt tokens. Figure 11 visualizes the $k - \epsilon$ results, the relationship between base loss and prompt length, and the most frequently observed tokens in the optimized control prompts. While the "exclusion zone" behavior (cf Figures 9, 6) is observed in the base loss vs. prompt length subplot, base loss remains a poor predictor of required prompt length. Moreover, Figure 4 reveals an even more uniform relationship between the initial rank of the target output token and the required prompt length.

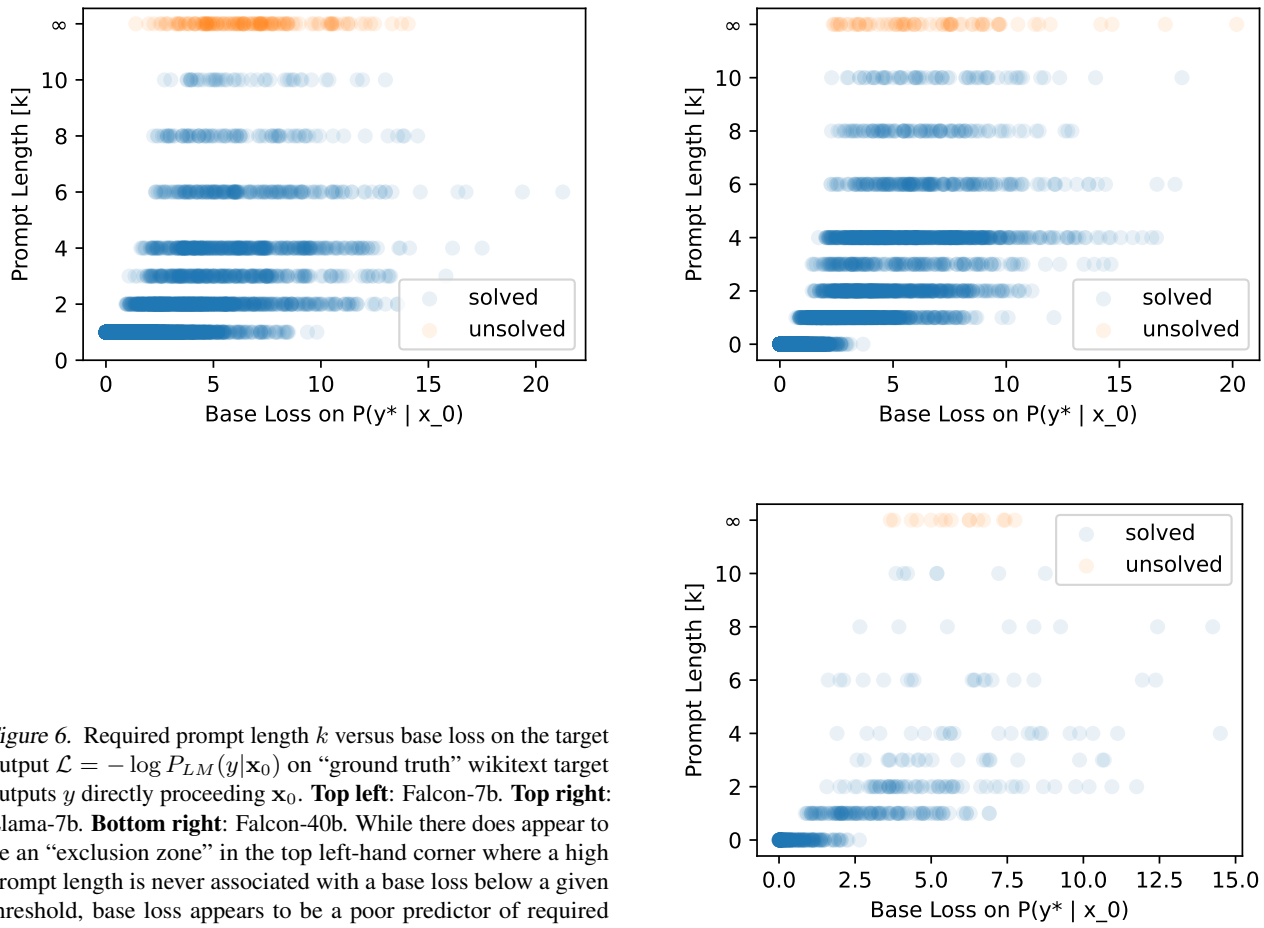

Figure 6. Required prompt length k versus base loss on the target output $\mathcal{L} = -\log P_{LM}(y|\mathbf{x}_0)$ on "ground truth" wikitext target outputs y directly proceeding $\mathbf{x}_0$. **Top left**: Falcon-7b. **Top right**: Llama-7b. **Bottom right**: Falcon-40b. While there does appear to be an "exclusion zone" in the top left-hand corner where a high prompt length is never associated with a base loss below a given threshold, base loss appears to be a poor predictor of required prompt length.

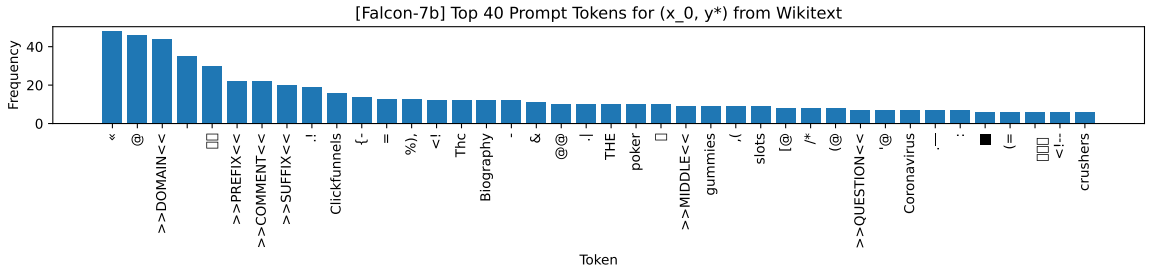

(a) Falcon-7b

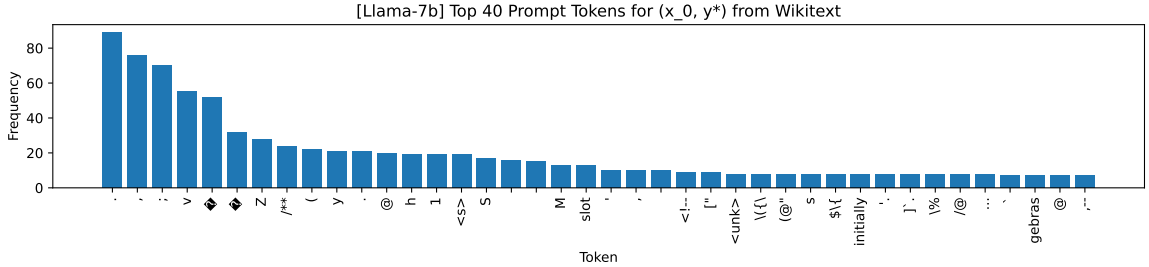

(b) Llama-7b

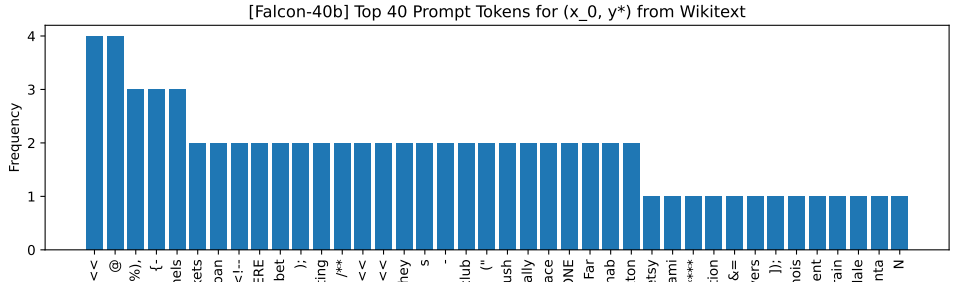

(c) Falcon-40b

Figure 7. Prompt token frequencies for Falcon-7b (top), Llama-7b (middle), and Falcon-40b (bottom) from Wikitext ground truth target token $k - \epsilon$ controllability experiments.

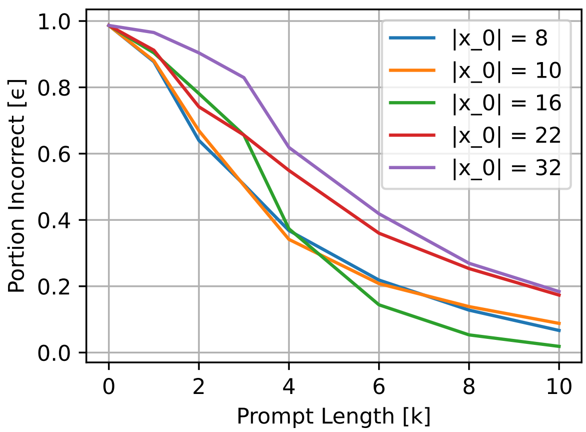

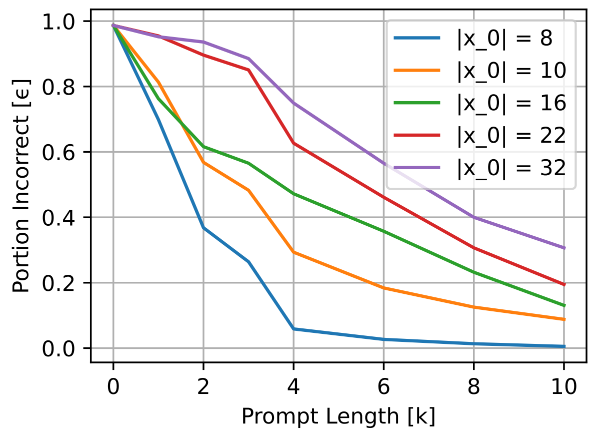

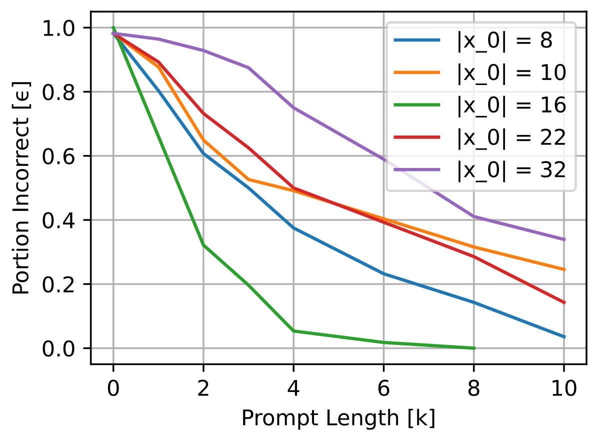

Figure 8. $k - \epsilon$ controllability plots on the top 75 most likely output tokens.
Top left: $k - \epsilon$ values for Falcon-7b. With $k = 10$ control tokens, 89.387% of the top 75 output tokens were reachable.
Top right: $k - \epsilon$ values for Llama-7b. With $k = 10$ control tokens, 85.493% of the top 75 output tokens were reachable.
Bottom right: $k - \epsilon$ values for Falcon-40b. With $k = 10$ control tokens, 85.714% of the top 75 output tokens were reachable.

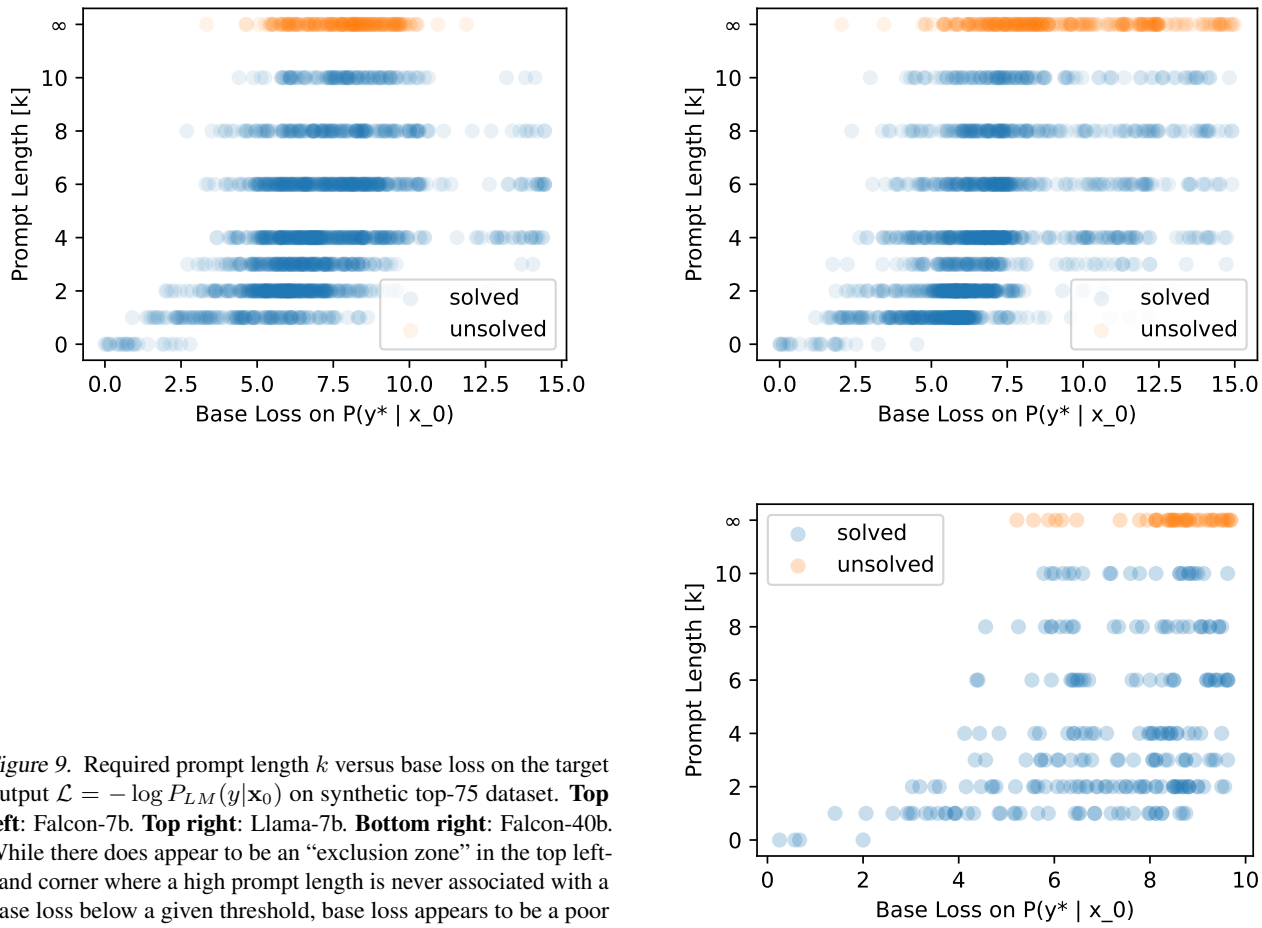

Figure 9. Required prompt length k versus base loss on the target output $\mathcal{L} = -\log P_{LM}(y|\mathbf{x}_0)$ on synthetic top-75 dataset. **Top left**: Falcon-7b. **Top right**: Llama-7b. **Bottom right**: Falcon-40b. While there does appear to be an "exclusion zone" in the top left-hand corner where a high prompt length is never associated with a base loss below a given threshold, base loss appears to be a poor predictor of required prompt length.

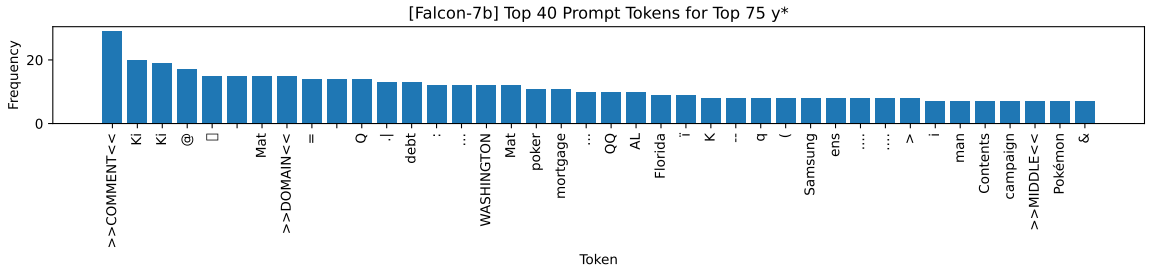

(a) Falcon-7b

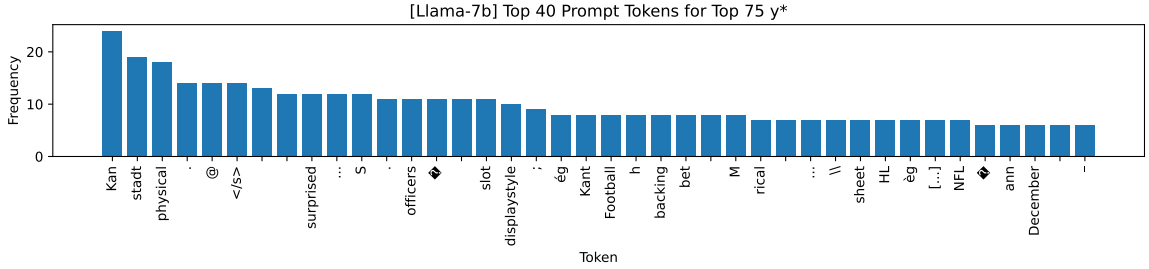

(b) Llama-7b

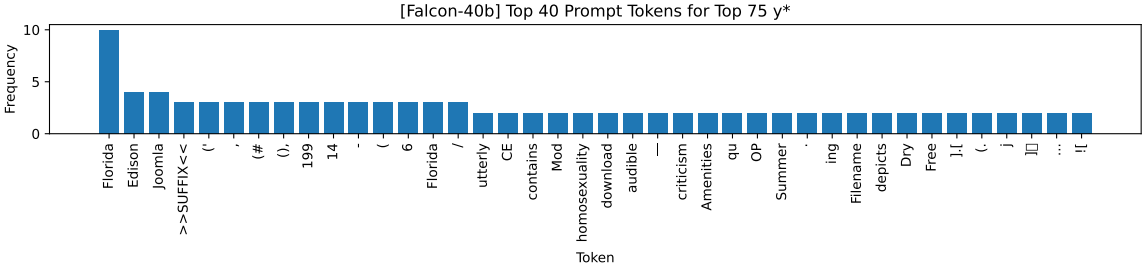

(c) Falcon-40b

Figure 10. Prompt token frequencies for Falcon-7b (top), Llama-7b (middle), and Falcon-40b (bottom) from Wikitext top-75 synthetic dataset $k - \epsilon$ controllability experiments.

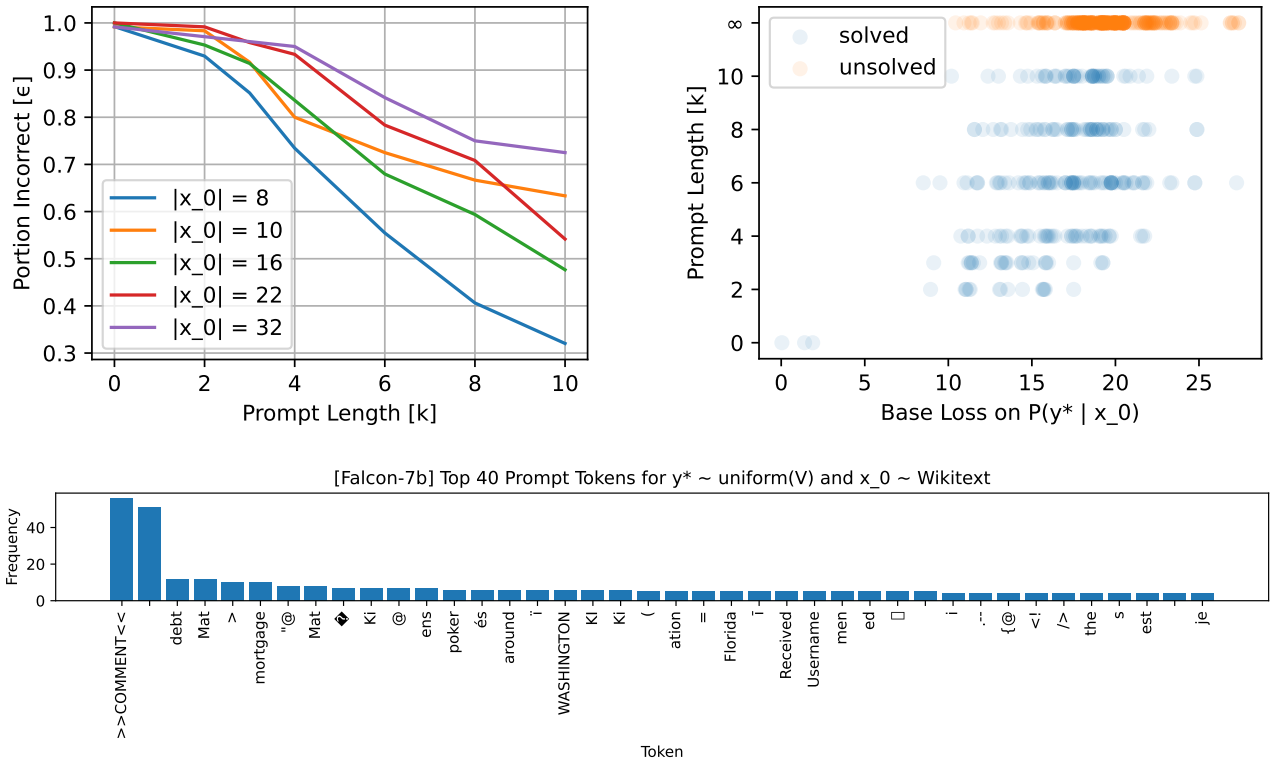

Figure 11. Supplementary figures on uniformly sampled target output controllability tests on Falcon-7b. **Top Left:** $k - \epsilon$ plot (46.42% controllable at $k = 10$). **Top Right:** Base loss versus required prompt length. **Bottom:** Histogram of top 40 most frequent tokens in optimized control prompts.